



Open Access : : ISSN 1847-9286

www.jESE-online.org

Original scientific paper

Electrochemical treatment of Acid Red 1 by electro-Fenton and photoelectro-Fenton processes

Camilo González-Vargas, Ricardo Salazar[✉] and Ignasi Sirés*[✉]

Laboratorio de Electroquímica Medio Ambiental, LEQMA, Departamento de Ciencias del Ambiente, Facultad de Química y Biología, Universidad de Santiago de Chile, USACH, Casilla 40, Correo 33, Santiago, Chile

*Laboratori d'Electroquímica dels Materials i del Medi Ambient, Departament de Química Física, Facultat de Química, Universitat de Barcelona, Martí i Franquès 1-11, 08028 Barcelona, Spain

[✉]Corresponding Author: E-mail: ricardo.salazar@usach.cl; Tel.: +56-2-27181134

[✉]Corresponding Author: E-mail: i.sires@ub.edu; Tel.: +34-93-4039243; Fax: +34-93-4021231

Received: July 23, 2014; Published: December 6, 2014

Abstract

Small volumes (100 mL) of acidic aqueous solutions with 30-200 mg L⁻¹ TOC of the toxic azo dye Acid Red 1 (AR1) have been comparatively treated by various electrochemical advanced oxidation processes (EAOPs). The electrolytic system consisted of a BDD anode able to produce [•]OH and an air-diffusion cathode that generated H₂O₂, which subsequently reacted with added Fe²⁺ to yield additional [•]OH from Fenton's reaction. Under optimized conditions (i.e., 1.0 mM Fe²⁺, 60 mA cm⁻², pH 3.0, 35 °C), the analysis of the initial rates for decolourization and AR1 decay assuming a pseudo-first-order kinetics revealed a much higher rate constant for photoelectro-Fenton (PEF, ~ 2.7x10⁻³ s⁻¹) compared to electro-Fenton (EF, ~ 0.6x10⁻³ s⁻¹). Mineralization after 180 min was also greater in the former treatment (90 % vs 63 %). The use of UV radiation in PEF contributed to Fe(III) photoreduction as well as to photodecarboxylation of refractory intermediates, yielding a mineralization current efficiency as high as 85% during the treatment of solutions of 200 mg L⁻¹ TOC. Primary reaction intermediates included three aromatic derivatives with the initial naphthalenic structure and four molecules only featuring benzenic rings, which were totally mineralized in PEF.

Keywords

Air-diffusion cathode; Azophloxine; boron-doped diamond (BDD); E128; EAOPs; decolourization; food azo dye; mineralization; Red 2G

Introduction

In recent years, great attention has been paid to the electrochemical advanced oxidation processes (EAOPs) based on Fenton's reaction chemistry for water decontamination [1]. Among them, electro-Fenton (EF) and photoelectro-Fenton (PEF) have been the most studied methods for the treatment of waters polluted by organic pollutants such as pharmaceuticals [2-4], pesticides [5-7] and synthetic dyes [8-11] due to their outstanding performance. In EF and PEF, H₂O₂ is continuously electrogenerated in the reaction cell from the two-electron reduction of injected or flushed gaseous O₂ as follows [1]:



The use of carbonaceous cathodes, particularly in the form of gas-diffusion electrodes (GDEs), promotes the production of a high yield of H₂O₂ at high rate. Therefore, the current efficiency for reaction (1) on GDEs turns out to be the highest among all tested materials. The activation of H₂O₂, which is a weak oxidant, is achieved in the presence of a small amount of metal catalyst, especially Fe²⁺, at pH around 3. Under such conditions, [•]OH is produced in the bulk from Fenton's reaction (2) [1]:



In PEF, the contaminated acidic solution is irradiated with artificial UV light, thus causing: (i) the photoreduction of Fe(OH)²⁺, which is the main Fe³⁺ species at pH 3, via photo-Fenton's reaction (3), and (ii) the photodecarboxylation of some Fe(III)-carboxylate complexes, which are quite refractory to oxidation by [•]OH formed from Fenton's reaction, via reaction (4) [1]. While reaction (3) contributes to form additional [•]OH as well as to maintain the Fenton's cycle by continuously regenerating Fe²⁺, reaction (4) makes it possible to reach great mineralization degrees.



For some pollutants, the performance of EF and PEF can be further enhanced by using a large O₂-overpotential anode such as boron-doped diamond (BDD). This material favours the electro-oxidation (EO) of the organic molecules by action of [•]OH adsorbed on the anode surface via reaction (5) [12]:



Acid Red 1 (AR1, also called Amido Naphtol Red G, Red 2G, Food Red 10 or Azophloxine, see chemical structure in Table 1) is a synthetic monoazo dye. Azo dyes constitute the most comprehensive and varied family among all synthetic organic dyes available in the industry for dyeing all kinds of fabrics [13]. Until 2007, AR1 was the preferred dye for baby food colouring due to the resulting intense red colour, but the Scientific Panel of the European Food Safety Authority (EFSA) on food additives, flavourings, processing aids and materials in contact with food was then asked to re-evaluate this dye due to food safety concerns related to its high toxicity and carcinogenic effects [14]. Based on this report, the European Union has agreed with its suspension as food colouring, as published in the Official Journal [15]. Not surprisingly, it is also banned in other countries outside Europe.

At present, it is known that AR1 is extensively metabolized to aniline, it may interfere with blood haemoglobin and it is suspected of being a carcinogen [16]. It is therefore one of the dyes

that the hyperactive children's support group recommends to be eliminated from the diet of children. In contrast, AR1 has become one the most used dyes in Chile and over the world for dyeing polyester-, nylon-, cellulose- and acrylic-based fibers. Consequently, if such industrial wastewaters are not conveniently treated before discharge, their impact on the surrounding ecosystems may be dramatic.

Some few studies have focused on the fate of AR1 upon application of non-electrochemical advanced oxidation processes (AOPs) [17-19]. Regarding the electrochemical technology, only its electrochemical reduction on an activated carbon fiber cathode has been reported [20], but as far as we are concerned its removal by EF and PEF with BDD or other anodes has not been reported yet. These latter processes are of great interest for the removal of food azo dyes, as some of us recently demonstrated for the treatment of Tartrazine solutions [21].

In this work, the decolourization, AR1 decay and mineralization profiles resulting from the treatment of synthetic aqueous solutions of 100 mL of AR1 by several EAOPs have been investigated. BDD and GDE, both of 2.5 cm², have been used at constant current upon addition of 50 mM Na₂SO₄ as supporting electrolyte at pH 3. The optimization of iron catalyst concentration and applied current has preceded the treatment of solutions with up to 200 mg L⁻¹ TOC content by PEF. In addition, chromatographic analyses allowed the identification of aliphatic and cyclic by-products formed during the cleavage of the AR1 structure.

Experimental

Chemicals

AR1 (disodium 8-acetamido-1-hydroxy-2-phenylazonaphthalene-3,6-disulfonate, C₁₈H₁₃N₃Na₂O₈S₂, Cl 18050, 60% purity) was purchased from Sigma-Aldrich. Anhydrous sodium sulfate used as background electrolyte and iron(II) sulfate heptahydrate used as catalyst in EF and PEF were of analytical grade from Merck. Solutions were prepared with bidistilled water and their pH was adjusted to 3 before the electrolyses with analytical grade sodium hydroxide or sulfuric acid from Merck. Other chemicals were obtained from Merck and Sigma-Aldrich.

Electrolytic system

The electrolyses were performed in an open, undivided cell containing a 100 mL solution and featuring a double jacket for circulation of external thermostated water at 35 °C (WiseCircu[®] WCB-11 water bath). The solution was stirred with a magnetic bar at 800 rpm to ensure good mixing and transport of reactants. The cell contained a 2.5 cm² Si/BDD thin-film electrode from Adamant[®] (500 ppm B) as the anode and a 2.5 cm² carbon-PTFE air-diffusion cathode from Electrocell[®]. The cathode was fed with compressed air flowing at 1 L min⁻¹ for H₂O₂ generation. The trials were performed at constant current provided by an MCP M10-QD305 power supply. In PEF, the solution was irradiated with a Black Ray B100AP lamp.

Equipment and analytical procedures

The solution pH was measured on an Extech 321990 pH-meter. Samples withdrawn at regular time intervals from electrolyzed solutions were neutralized at pH 7-8 to stop the degradation process and filtered with 0.45 µm PTFE filters from Whatman before analysis. The decolourization of AR1 solutions was monitored from the absorbance (A) decay at the maximum visible wavelength (λ_{\max}) of 520 nm, measured from the spectra recorded on a Cary 1E UV/Vis spectrophotometer (Varian). The percentage of colour removal or decolourization efficiency was then determined as follows [21]:

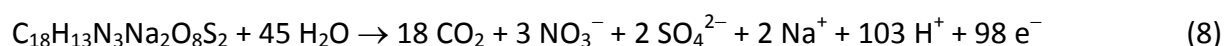
$$\text{Colour removal, \%} = 100 \frac{A_0 - A_t}{A_0} \quad (6)$$

where A_0 and A_t denote the absorbance at initial time and after an electrolysis time t , respectively.

The mineralization of solutions was monitored from their total organic carbon (TOC) abatement, determined on a Vario TOC Select analyzer. From these data, the mineralization current efficiency (MCE) at a given current (I / A) and electrolysis time (t / h) were estimated as follows [1]:

$$\text{MCE, \%} = 100 \frac{nFV_s \Delta(\text{TOC})_{\text{exp}}}{4.32 \times 10^7 mIt} \quad (7)$$

where F is the Faraday constant (96487 C mol^{-1}), V_s is the solution volume (L), $\Delta(\text{TOC})_{\text{exp}}$ is the experimental TOC decay (mg L^{-1}), 4.32×10^7 is a conversion factor ($3600 \text{ s h}^{-1} \times 12000 \text{ mg mol}^{-1}$) and m is the number of carbon atoms of AR1 (18 atoms). The number of electrons (n) consumed per each dye molecule was taken as 98 considering that its mineralization leads to carbon dioxide and nitrate and sulfate ions as follows:



AR1 decay was followed by reversed-phase high performance liquid chromatography (HPLC) with a Waters 625 LC fitted with a Hibar® RP-18e 5 μm , 150 \times 4 mm, column at 25 °C and coupled with a photodiode array detector set at $\lambda = 520 \text{ nm}$. The mobile phase was a 70:30 (v/v) acetonitrile/1.0 mM ammonium acetate (pH 4) mixture at 0.5 mL min^{-1} . Generated carboxylic acids were detected by ion-exclusion HPLC using the same LC fitted with a Bio-Rad Aminex HPX 87H, 300 \times 7.8 mm, column at 25 °C and setting the array detector at $\lambda = 210 \text{ nm}$. The isocratic elution at 0.6 mL min^{-1} with 4 mM H_2SO_4 as the mobile phase yielded good peaks for maleic ($t_r = 8.8 \text{ min}$), oxamic ($t_r = 10.6 \text{ min}$), malic ($t_r = 11.3 \text{ min}$), formic ($t_r = 14.9 \text{ min}$) and acetic ($t_r = 16.1 \text{ min}$).

The cyclic and/or aromatic intermediates were analyzed by gas chromatography coupled to mass spectrometry (GC-MS). Several electrolyses were carried out under different experimental conditions for short and long times. The final solutions were collected together until reaching 500 mL, which were then extracted three times with 30 mL CH_2Cl_2 . The resulting organic solution (90 mL) was dried with anhydrous Na_2SO_4 , then filtered and completely evaporated in a rotary to obtain a pale yellow solid that was further analyzed.

Results and Discussion

Influence of the experimental parameters on the degradation of Acid Red 1 by EF process

Solutions containing 300 mg L^{-1} AR1 (i.e., 0.59 mM AR1 or 100 mg L^{-1} TOC) were electrolyzed at 60 mA cm^{-2} in the presence of different amounts of Fe^{2+} as catalyst. As can be seen in Fig. 1, the absence of Fe^{2+} (so-called EO process) caused the slowest decolourization and TOC abatement, only reaching 70 % colour removal after 70 min and 25 % TOC decay after 180 min. Under the present EO conditions, given the weak oxidation power of H_2O_2 , the organic matter can be mainly degraded by BDD($\bullet\text{OH}$) formed via reaction (5). This radical tends to be very active towards the initial pollutants and their by-products because it is weakly physisorbed on the anode surface and it is generated at a very positive potential. Moreover, it is known that hydroxyl radicals can react at high rate with all double bonds in the aromatic rings and, especially, with the $-\text{N}=\text{N}-$ bond. However, since BDD($\bullet\text{OH}$) is confined to the anode vicinity, the degradation process becomes

severely limited by mass transport, thus being needed a much longer electrolysis time to effectively destroy the molecules in a batch system without recirculation like the one tested here.

In contrast to the previous finding, within the same time period the presence of Fe^{2+} allowed the complete decolourization as well as a greater mineralization in all cases, which can be accounted for by the crucial contribution of $\cdot\text{OH}$ formed in the bulk from Fenton's reaction (2). As can be seen in Fig. 1a, the increase in Fe^{2+} concentration from 0.1 to 0.5 and then to 1.0 mM clearly accelerated the colour removal, being necessary 70, 60 and 40 min, respectively, to get colourless solutions.

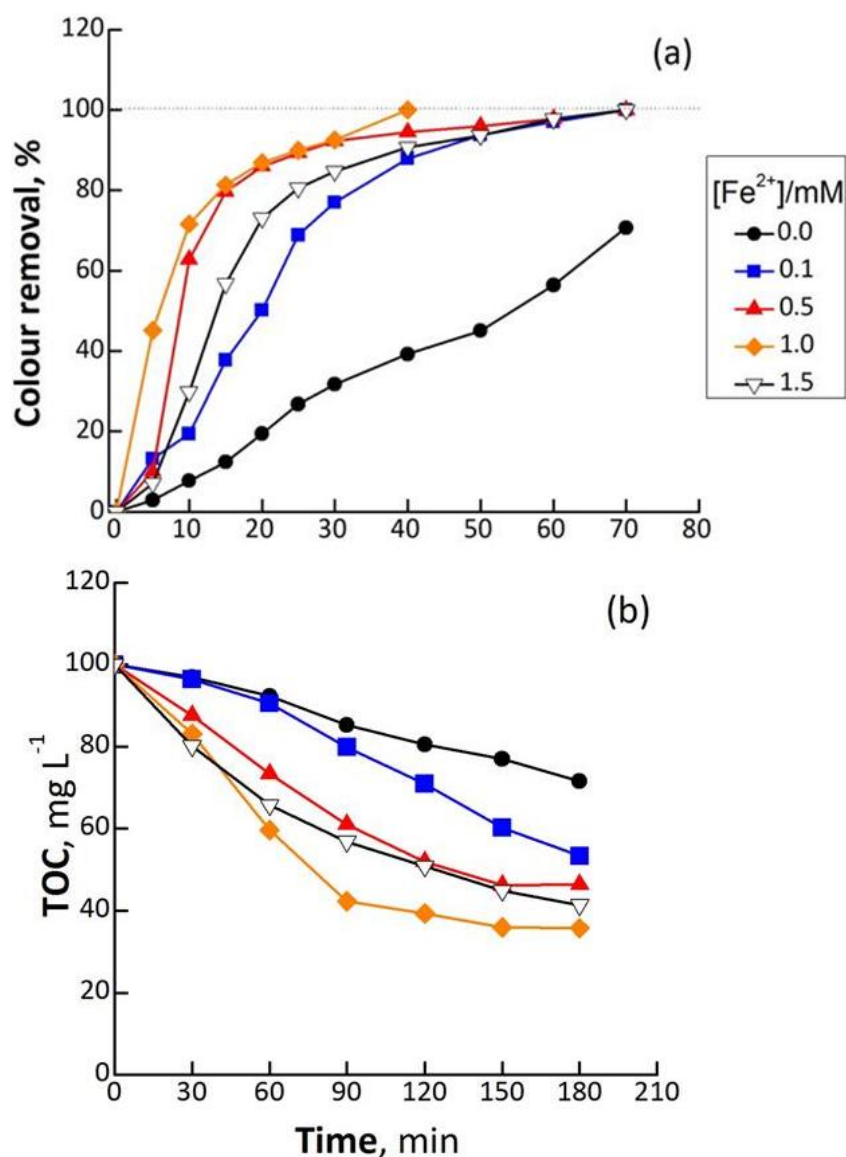


Figure 1. Effect of Fe^{2+} concentration on (a) decolourization efficiency at 520 nm and (b) TOC removal with electrolysis time for the electro-Fenton treatment of solutions of 300 mg L^{-1} AR1 in $0.05 \text{ M Na}_2\text{SO}_4$ at pH 3.0, $35 \text{ }^\circ\text{C}$ and 60 mA cm^{-2} .

The rising catalyst content had a positive effect on the mineralization profiles as well, since 47, 54 and 63 % TOC removal was attained after 180 min using 0.1, 0.5 and 1.0 mM Fe^{2+} . In contrast, further increase to 1.5 mM was detrimental, eventually leading to slower colour removal and only 59 % TOC abatement at 180 min. This phenomenon can be mainly explained by the larger extent of parasitic reactions causing the consumption of $\cdot\text{OH}$, particularly by Fe^{2+} . It must be noted that the mineralization was always partial, with a tendency to reach a plateau owing to the plausible

accumulation of refractory intermediates (as confirmed later on) that could not be oxidized by $\bullet\text{OH}$ in the bulk and were very slowly destroyed by BDD($\bullet\text{OH}$). In conclusion, 1.0 mM was chosen as the optimum Fe^{2+} concentration for subsequent tests.

The effect of current density within the range 8-80 mA cm^{-2} , carried out under conditions shown in Fig. 1 with 1 mM Fe^{2+} as the optimized amount, is depicted in Fig. 2. These trials aimed at exploring the possibility of enhancing the decolourization and mineralization kinetics, which is based on the fact that the applied current determines the yield of BDD($\bullet\text{OH}$) formed via reaction (5) as well as that of $\bullet\text{OH}$ via reaction (2) because it depends on the H_2O_2 formation rate and Fe^{2+} regeneration rate.

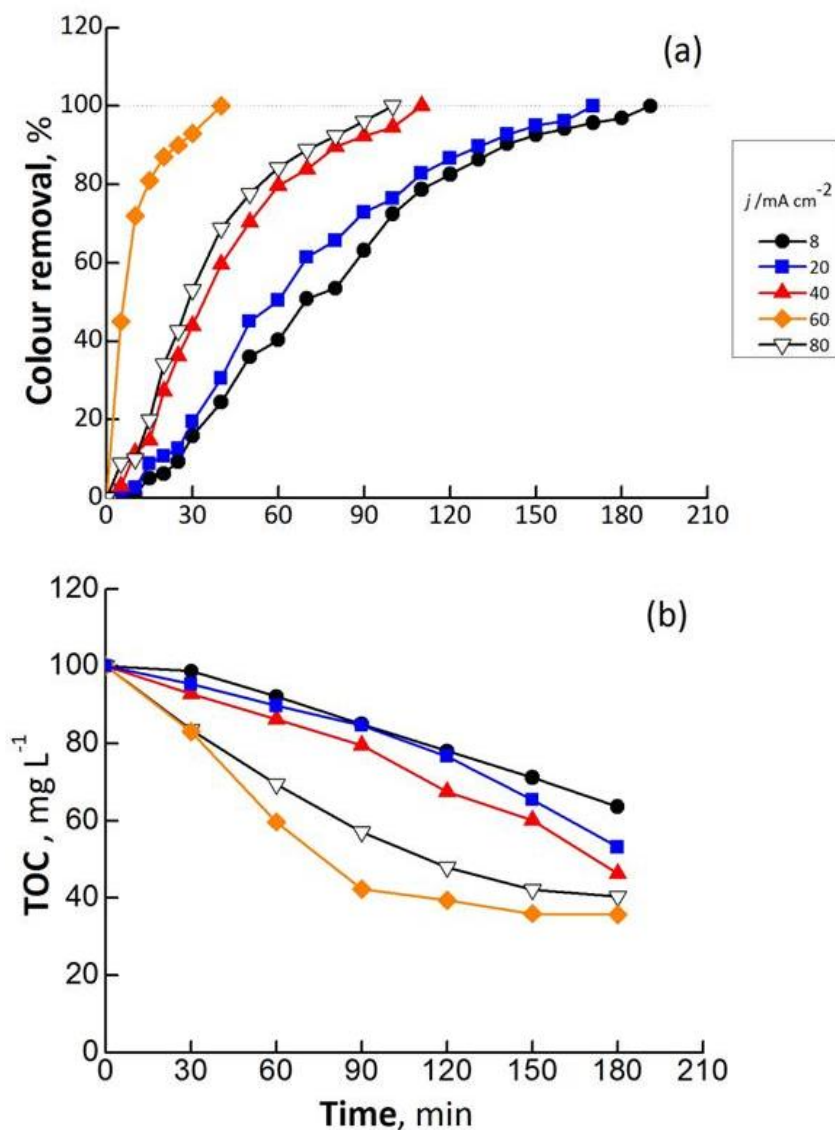


Figure 2. Effect of current density on (a) decolourization efficiency at 520 nm and (b) TOC removal with electrolysis time for the electro-Fenton treatment of solutions of 300 mg L⁻¹ AR1 in 0.05 M Na_2SO_4 with 1.0 mM Fe^{2+} at pH 3.0 and 35 °C.

A progressive increase in current density from 8 to 60 mA cm^{-2} caused the acceleration of both, decolourization and mineralization. This can be easily explained by the faster generation of BDD($\bullet\text{OH}$) on the anode and $\bullet\text{OH}$ in the bulk. Note that even the lowest current densities were able to yield the complete decolourization at long electrolysis time. However, further increase to 80 mA cm^{-2} was detrimental since it caused a slower colour removal and led to a lower TOC

removal. This negative effect arises from the shift in cathode potential to unfavourable values that promoted the reduction of O_2 to H_2O over reaction (1) and hindered the conversion of Fe^{3+} to Fe^{2+} . As a matter of fact, H_2O_2 concentration analyzed during the electrolyses at 60 and 80 $mA\ cm^{-2}$ reached 25 mM and 15 mM, respectively. Thus, 60 $mA\ cm^{-2}$ was chosen as the optimum value.

Effect of UVA light

As discussed in the Introduction, for most of the contaminated solutions studied in the past it was possible to enhance the degradation process by irradiating them with UV light, which favoured the oxidation of pollutants and their by-products due to the action of reaction (3) and (4). In the present study, no direct photolysis of AR1 by UV light was observed, since its peak during the HPLC analyses remained unchanged. This ensured the photostability of AR1 during the electrolyses run under PEF conditions. For this purpose, the AR1 solutions were treated as done in the previous EF experiments but incorporating the UV lamp near the cell.

As shown in Fig. 3a, solutions of 300 $mg\ L^{-1}$ AR1 treated by PEF under the optimized conditions described before (*i.e.*, 1.0 mM Fe^{2+} and 60 $mA\ cm^{-2}$) were more quickly decolourized compared to EF trials, being required 50 min instead of 60 min to become colourless (see Fig. 1a for comparison). The key contribution of photoreduction reaction (3) favoured the faster regeneration of Fe^{2+} , which then was able to accelerate the production of $\bullet OH$ from reaction (2). On the other hand, PEF also yielded a much larger mineralization after 180 min, reaching 90 % owing to photodecarboxylation reaction (4). As reported elsewhere [1], some of the reaction intermediates can form stable complexes with Fe(III) that can be effectively degraded only upon action of UV photons since $\bullet OH$ and BDD($\bullet OH$) are much less effective. Fig. 3a also depicts the decay of AR1 monitored by HPLC during the same experiment. Its profile is quite similar to colour removal profile, which means that no other coloured by-products were formed during the treatment. Assuming a pseudo-first-order kinetics, an apparent rate constant (k_{app}) of $2.74 \times 10^{-3}\ s^{-1}$ for AR1 decay was determined. The decay of the dye was also similar to the colour removal trend for EF treatment (not shown), revealing a much smaller $k_{app} = 0.59 \times 10^{-3}\ s^{-1}$. Therefore, the beneficial synergy between $\bullet OH$, BDD($\bullet OH$) and UV light for the decontamination of AR1 solutions is demonstrated.

Due to production needs, actual wastewaters may present a significant variation in the dye content over time and thus, it is mandatory that the water treatment technology is flexible enough to be adapted to such changes. The effect of AR1 concentration on the mineralization profile *vs.* time is shown in Fig. 3b. A similar TOC removal was attained after 180 min for solutions containing 30 and 100 $mg\ L^{-1}$ TOC. In contrast, only 75 % mineralization was reached for solutions with 200 $mg\ L^{-1}$ TOC, which is simply due to the much larger number of organic molecules to be degraded in the latter case. But, an important feature to be highlighted is the progressively increasing slope of the curves (*i.e.*, larger mineralization rate) upon increase of AR1 concentration, which can be related to the more efficient reaction between $\bullet OH$ /BDD($\bullet OH$) and the organic molecules. Indeed, low AR1 concentrations cause the waste of radicals in self-destruction and other side reactions, whereas high organic contents lead to effective oxidation reactions. This is clearly demonstrated in Fig. 3c, which compares the evolution of MCE *vs.* time for several EAOPs. For solutions with 100 $mg\ L^{-1}$ TOC, the efficiency increases in the sequence $EO < EF < PEF$, with maximum values of 10, 25 and 55 %, respectively. As discussed before, this can be related to the more favorable synergy between different oxidants in the case of PEF. In addition, a greater MCE resulted from the treatment of larger AR1 concentrations in PEF, reaching 85 % during the

treatment of 200 mg L⁻¹ TOC, thus confirming the lower extent of parasitic reactions that cause radical waste. Note that MCE tends to decrease at long electrolyses time, which can be explained by (i) the formation of more resistant intermediates and (ii) the mass transport limitations related to low organic loads.

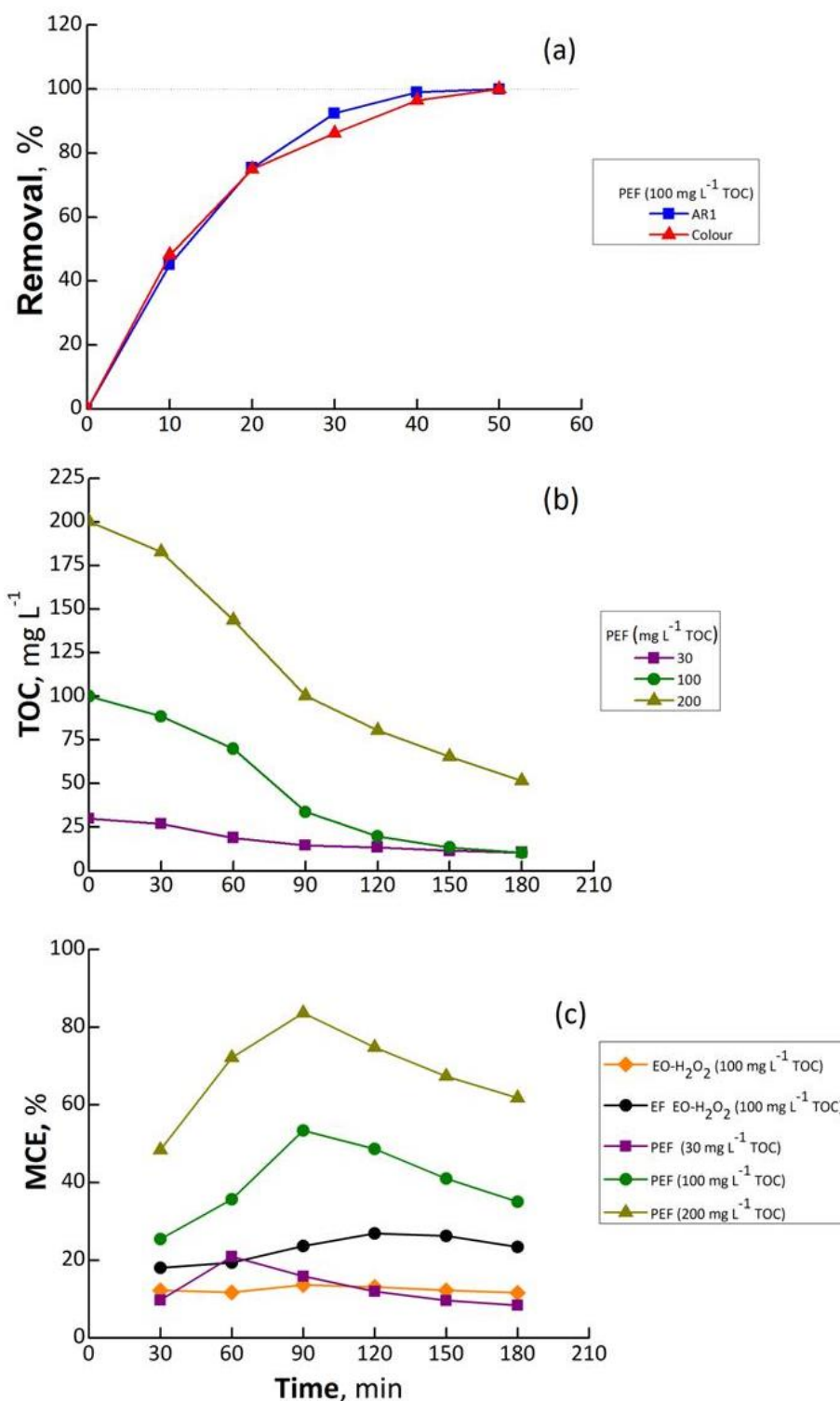
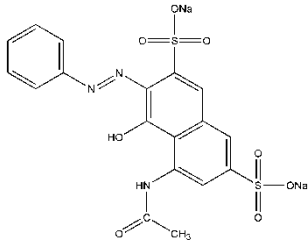
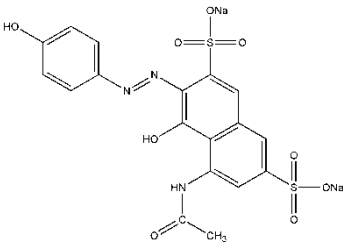
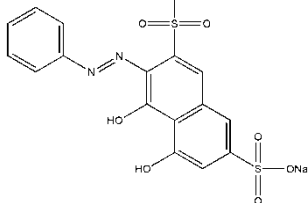
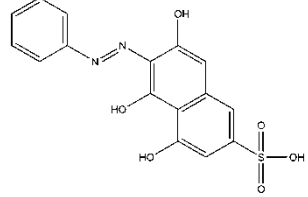
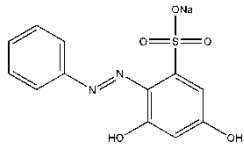
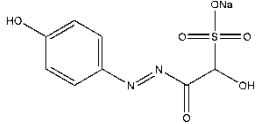
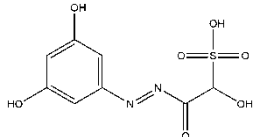


Figure 3. (a) Decolourization efficiency at 520 nm and percentage of AR1 removal with electrolysis time for the photoelectro-Fenton treatment of solutions of 300 mg L⁻¹ AR1 in 0.05 M Na₂SO₄ with 1.0 mM Fe²⁺ at pH 3.0, 35 °C and 60 mA cm⁻². (b) TOC abatement vs. time for the same experiment compared to trials at different AR1 concentrations. (c) MCE for trials shown in (b) compared to EO (0 mM Fe²⁺) and EF (1.0 mM Fe²⁺) treatments shown in Fig. 1b.

Identification of reaction intermediates

Table 1 summarizes the seven aromatic intermediates identified during PEF treatments.

Table 1. Structures of Acid Red 1 and its degradation intermediates identified by GC-MS analysis.

Chemical name	Structure	m/z
<u>Acid Red 1</u>		509.42
<u>Naphthalene derivatives</u>		
Disodium 8-acetamido-1-hydroxy-2-(4-hydroxyphenylazo)naphthalene-3,6-disulfonate		524.12
Disodium 1,2-dihydroxy-3-phenylazonaphthalene-4,7-disulfonate		468.37
(5-Phenylazo-3,4,6-trihydroxynaphthalene)sulfonic acid		362.33
<u>Benzene derivatives</u>		
Sodium (3,5-dihydroxy-2-phenylazo)benzenesulfonate		316.26
Sodium (1-hydroxy-2-[4-hydroxyphenylazo]-2-oxo)ethanesulfonate		282.21
2-(3,5-dihydroxyphenylazo)-1-hydroxy-2-oxoethanesulfonic acid		276.22
Hydroquinone		110.11

As can be seen, $\cdot\text{OH}$ and BDD($\cdot\text{OH}$) led to the hydroxylation of the benzenic and naphthalenic rings of AR1 to yield three naphthalene derivatives. The subsequent action of radicals onto AR1 and/or onto those intermediates led to the formation of four benzene derivatives. The accumulation of these aromatic intermediates would be dangerous due to their inherent high toxicity and thus, PEF treatments had to be prolonged until their complete disappearance.

The progressive cleavage and oxidation of the aromatic intermediates gave rise to the formation of short-chain aliphatic carboxylic acids, as also described elsewhere for other pollutants [22]. Five C_1 - C_4 acids were identified by ion-exclusion HPLC, namely maleic, oxamic, malic, formic and acetic. As explained from Fig. 3, PEF ensured the almost complete removal of all these acids since the TOC in the final solutions was <10 % after 180 min.

Conclusions

PEF technology is confirmed as a very powerful alternative for giving response to environmental concerns related to water contamination by organic pollutants. This process allows a much faster destruction of AR1 as well as a more significant and efficient TOC removal compared to EO and EF, thus becoming a promising technology for the treatment of industrial wastewaters containing this azo dye. The toxic intermediates formed during the first degradation stages are completely transformed into aliphatic molecules, which are slowly converted to CO_2 and H_2O . The use of renewable energy such as sunlight in sunny countries like Chile and Spain, giving rise to the so-called solar photoelectro-Fenton (SPEF) process, would be an interesting feature for real-scale application.

Acknowledgements: The authors thank CONICYT (Chile) for support under FONDECYT grant 1130391 and DICYT-USACH, as well as for the PhD fellowship N° 21130071 awarded to C. González-Vargas.

References

- [1] E. Brillas, I. Sirés, M. A. Oturan, *Chemical Reviews* **109** (2009) 6570–6631
- [2] A. Dirany, S. Efremova Aaron, N. Oturan, I. Sirés, M. A. Oturan, J. J. Aaron, *Analytical and Bioanalytical Chemistry* **400** (2011) 353–360
- [3] A. El-Ghenymy, N. Oturan, M. A. Oturan, J.A. Garrido, P. L. Cabot, F. Centellas, R. M. Rodríguez, E. Brillas, *Chemical Engineering Journal* **234** (2013) 115–123
- [4] S. Loaiza-Ambuludi, M. Panizza, N. Oturan, A. Özcan, M. A. Oturan, *Journal of Electroanalytical Chemistry* **702** (2013) 31–36
- [5] N. Oturan, M. Zhou, M. A. Oturan, *Journal of Physical Chemistry A* **114** (2010) 10605–10611
- [6] R. Salazar, M. S. Ureta-Zañartu, *Water Air Soil Pollution* **223** (2012) 4199–4207
- [7] J. Urzúa, C. González-Vargas, F. Sepúlveda, M. S. Ureta-Zañartu, R. Salazar, *Chemosphere* **93** (2013) 2774–2781
- [8] M. Zhou, Q. Yu, L. Lei, *Dyes and Pigments* **77** (2008) 129–136
- [9] M. Panizza, M. A. Oturan, *Electrochimica Acta* **56** (2011) 7084–7087
- [10] E. J. Ruiz, A. Hernández-Ramírez, J. M. Peralta-Hernández, C. Arias, E. Brillas, *Chemical Engineering Journal* **171** (2011) 385–392
- [11] R. Salazar, E. Brillas, I. Sirés, *Applied Catalysis B: Environmental* **115-116** (2012) 107–116
- [12] M. Panizza, G. Cerisola, *Chemical Reviews* **109** (2009) 6541–6569
- [13] C. A. Martínez-Huitle, E. Brillas, *Applied Catalysis B: Environmental* **87**(2009) 105–145
- [14] European Food Safety Authority, *The EFSA Journal* **515** (2007) 1-28

- [15] Official Journal of the European Union L 195/8, 27.7.2007. Commission regulation (EC) No 884/2007 of July 2007 on emergency measures suspending the use of E 128 Red 2G as food colour
- [16] A. F. Villa, F. Conso, *EMC - Toxicologie-Pathologie* **1** (2004) 161-177
- [17] Cs. M. Földváry, L. Wojnárovits, *Radiation Physics and Chemistry* **78** (2009) 13–18
- [18] N. K. Daud, M.A. Ahmad, B.H. Hameed, *Chemical Engineering Journal* **165** (2010) 111–116
- [19] S. Thomas, R. Sreekanth, V. A. Sijumon, U. K. Aravind, C. T. Aravindakumar, *Chemical Engineering Journal* **244** (2014) 473–482
- [20] Z. Shen, W. Wang, J. Jia, J. Ye, X. Feng, A. Peng, *Journal of Hazardous Materials* **B84** (2001) 107–116.
- [21] A. Thiam, M. Zhou, E. Brillas, I. Sirés, *Applied Catalysis B: Environmental* **150-151**(2014) 116–125
- [22] M. A. Oturan, M. Pimentel, N. Oturan, I. Sirés, *Electrochimica Acta* **54** (2008) 173–182